



# Notch1 Inhibits Rosiglitazone-Induced Adipogenic Differentiation in Primary Thymic Stromal Cells

Yajun Wang<sup>1</sup>, Jianxin Tan<sup>2</sup>, Hongmei Du<sup>3</sup>, Xue Liu<sup>1</sup>, Siliang Wang<sup>3</sup>, Simeng Wu<sup>4</sup>, Zhe Yuan<sup>4</sup> and Xike Zhu<sup>1\*</sup>

<sup>1</sup> Research Center, Shengjing Hospital of China Medical University, Shenyang, China, <sup>2</sup> State Key Laboratory of Reproductive Medicine, Department of Prenatal Diagnosis, The Affiliated Obstetrics and Gynecology Hospital of Nanjing Medical University, Nanjing Maternity and Child Health Care Hospital, Nanjing, China, <sup>3</sup> Department of Medical Oncology, Shengjing Hospital of China Medical University, Shenyang, China, <sup>4</sup> Department of Blood Transfusion, Shengjing Hospital of China Medical University, Shenyang, China

## OPEN ACCESS

### Edited by:

Giovanni Li Volti,  
Università degli Studi di Catania, Italy

### Reviewed by:

Wei Chen,  
Beijing Institute of Pharmacology &  
Toxicology, China  
Rossella Rota,  
Bambino Gesù Ospedale Pediatrico  
(IRCCS), Italy

### \*Correspondence:

Xike Zhu  
zhuxk@sj-hospital.org

### Specialty section:

This article was submitted to  
Experimental Pharmacology  
and Drug Discovery,  
a section of the journal  
Frontiers in Pharmacology

**Received:** 25 June 2018

**Accepted:** 18 October 2018

**Published:** 12 November 2018

### Citation:

Wang Y, Tan J, Du H, Liu X,  
Wang S, Wu S, Yuan Z and Zhu X  
(2018) Notch1 Inhibits  
Rosiglitazone-Induced Adipogenic  
Differentiation in Primary Thymic  
Stromal Cells.  
*Front. Pharmacol.* 9:1284.  
doi: 10.3389/fphar.2018.01284

Adipocyte deposition is believed to be a primary characteristic of age-related thymic involution. Herein, we cultured primary thymic stromal cells (TSCs), used rosiglitazone, a potent peroxisome proliferator-activated receptor  $\gamma$  (PPAR $\gamma$ ) agonist, to induce adipogenic differentiation, and investigated the differentially expressed genes during adipogenic differentiation by using RNA-sequencing analysis. Furthermore, the effects of Notch1 on rosiglitazone-induced adipogenic differentiation of TSCs as well as the underlying mechanisms were also investigated. As a result, we identified a total of 1737 differentially expressed genes, among which 965 genes were up-regulated and 772 genes were down-regulated in rosiglitazone-treated cells compared with control cells. Gene ontology (GO) enrichment analysis showed that the GO terms were enriched in metabolic process, intracellular, and protein binding. Kyoto encyclopedia of genes and genomes (KEGG) analysis showed that a number of pathways, including ubiquitin mediated proteolysis, PPAR signaling pathway, and mammalian target of rapamycin (mTOR) signaling pathway were predominantly over-represented. Meanwhile, overexpression of Notch1 suppressed and inhibition of Notch1 promoted rosiglitazone-induced adipogenic differentiation in TSCs, and the pro-adipogenic effects of the Notch inhibitor DAPT were associated with the activation of autophagy. Taken together, our results suggest that Notch1 is a key regulator in thymic adipogenesis and may serve as a potential target to hinder thymic adiposity in age-related thymic involution.

**Keywords:** thymic adipogenesis, thymic stromal cells, RNA-seq, Notch1, autophagy

## INTRODUCTION

The thymus is a unique primary lymphoid organ, which provides the inductive microenvironments to ensure the differentiation, development, and maturation of T cells (Chaudhry et al., 2016). Unlike most other organs, the thymus enlarges from infancy to adolescence but begins to slowly shrink from puberty onwards (Aw and Palmer, 2011). Termed as age-related involution, this

physiological process is characterized by decrease in thymic size, abnormal thymic architecture, and the replacement of thymic epithelial cells with adipocytes, eventually leading to decrease in naïve T cell output and increased risk to infection, autoimmune disease, and cancer in the elderly (Gui et al., 2012). Adipocyte deposition is believed to be a primary characteristic of age-related thymic involution and contributes to the deterioration of the thymic microenvironments (Flores et al., 1999; Ventevogel and Sempowski, 2013). Recent evidence suggests that the transdifferentiation of thymic stromal cells (TSCs) into adipocytes is a possible source of thymic adipogenesis (Youm et al., 2009; Tan J. et al., 2016). However, the underlying mechanisms involved in thymic adiposity remain to be clarified.

The next generation sequencing technology, a state-of-the-art, large-scale and systematic analysis, has been widely used in transcriptomic studies, termed as RNA-sequencing (RNA-seq), which enable us to simultaneously characterize 1000s of transcripts expressed in defined biological samples (Wang et al., 2009; McGettigan, 2013). Because of its advantages in high throughput and low cost, RNA-seq is rapidly replacing the microarray technology as the first choice for gene expression studies (Zhao et al., 2014). To the best of our knowledge, however, there have been no reports using RNA-seq analysis to identify key regulators in thymic adipogenesis.

Peroxisome proliferator-activated receptor  $\gamma$  (PPAR $\gamma$ ) is a key player in the differentiation of adipocytes, and constitutive PPAR $\gamma$  activation induces ectopic adipogenesis and promotes age-related thymic involution in mice (Youm et al., 2010; Ernszt et al., 2017). Furthermore, rosiglitazone, a potent PPAR $\gamma$  agonist, has been successfully used to induce adipogenic differentiation of OP9-DL1 cells and primary TSCs *in vitro* (Yang et al., 2009; Tan et al., 2017). In order to identify key regulators in thymic adipogenesis, we cultured primary TSCs, used rosiglitazone to induce adipogenic differentiation, and investigated the differentially expressed genes during adipogenic differentiation by using RNA-seq analysis. Furthermore, we found that Notch signaling pathway is involved in adipogenic differentiation of TSCs. Finally, we evaluated whether Notch1 inhibits rosiglitazone-induced adipogenic differentiation in TSCs and, if so, whether the effects of Notch1 are associated with the regulation of autophagy in TSCs.

## MATERIALS AND METHODS

### Animals and Chemicals

C57BL/6 mice at ages of 2–3 months were obtained from Huafukang Bioscience Co. Ltd. (Beijing, China) and housed under specific pathogen-free conditions in the animal care facility at Shengjing Hospital of China Medical University. All animal experiment protocols were reviewed and approved by the Animal Ethics Committee of Shengjing Hospital. The Notch inhibitor DAPT (N-[N-(3, 5-Difluorophenacetyl)-L-alanyl]-S-phenylglycine t-butyl ester) and autophagy inhibitor 3-methyladenine (3-MA) were purchased from MedChem Express (Monmouth Junction, NJ, United States).

### Cell Culture

Primary TSCs were cultured from postnatal thymi by enzymatic digestion. Briefly, freshly dissected thymic lobes were cut into small fragments and washed with RPMI-1640 medium to remove the majority of thymocytes. Then, the thymic fragments were incubated for 20 min at 37°C with RPMI-1640 medium containing 0.05% Liberase<sup>TH</sup> (Roche, Basel, Switzerland) and 200 U/ml DNase I (Sangon Biotechnology, Shanghai, China). Gentle mechanical agitation was performed, and the cell suspensions were collected and added into phosphate buffered saline (PBS) containing 0.5% bovine serum albumin (BSA) and 2 mM ethylenediaminetetraacetic acid (EDTA) to neutralize digestion. The remaining aggregates were further treated with enzymatic mixture, and the digestion was repeated thrice until completely dispersed. The cell suspensions were pooled, centrifuged, and resuspended in PBS solution. After filtered through 100  $\mu$ m mesh, the cells were seeded into 24-well plate at a density of 10<sup>6</sup>/well and cultured in DMEM/F12 medium supplemented with 3  $\mu$ g/ml insulin (Biovision, Livingston, NJ, United States), 20 ng/ml epidermal growth factor (PeproTech, Rocky Hill, NJ, United States), 100 U/ml penicillin, 100 g/ml streptomycin, and 20% fetal bovine serum (FBS; Biological Industries, Kibbutz Beit-Haemek, Israel) at 37°C in a 5% CO<sub>2</sub> incubator (Yang et al., 2009). After attachment, the thymocytes were removed by refreshing the culture medium. To induce adipogenic differentiation, TSCs at passage 3 were incubated with 10  $\mu$ M rosiglitazone (Aladdin, Shanghai, China) for 7 days, and the medium containing rosiglitazone was refreshed every other day. Dimethyl sulphoxide (DMSO)-treated cells were used as a vehicle control (Tan et al., 2017).

### RNA Extraction, Library Preparation for RNA-Seq

Total RNA was isolated by using RNAiso Plus (TAKARA, Dalian, China). The purity of RNA was assessed with a NanoPhotometer<sup>®</sup> spectrophotometer (IMPLEN, Westlake Village, CA, United States). RNA concentrations were measured by using Qubit<sup>®</sup> RNA Assay Kit on a Qubit 2.0 Fluorometer (Life Technologies, Carlsbad, CA, United States), and RNA integrity was evaluated by using RNA Nano 6000 Assay Kit on the Bioanalyzer 2100 system (Agilent Technologies). For library preparation, rRNA was depleted by using the EpicentreRibo-zero<sup>TM</sup> rRNA Removal Kit (Madison, WI, United States). Subsequently, fragmentation was performed in NEBNext first strand synthesis reaction buffer, and the first-strand cDNA was synthesized with a random hexamer primer and M-MuLV reverse transcriptase. DNA polymerase I and RNase H were used to synthesize the second-strand cDNA. After adenylation of the 3' ends of the DNA fragment, the NEBNext adaptor was ligated, and 150–200 bp cDNA fragments were purified. PCR amplification was carried out to enrich the cDNA libraries using Phusion high-fidelity DNA polymerase, universal PCR primers, and index primer. The quality of library was assessed with the Agilent bioanalyzer 2100 system. The libraries were sequenced on an Illumina HiSeq 4000 platform

(Illumina, San Diego, CA, United States), and 150 bp paired-end reads were obtained after clustering of the index-coded samples.

## Analysis of RNA-Seq Reads and Differentially Expressed Transcripts

Raw data in the Fastq format were analyzed by in-house perl scripts to obtain clean reads. The clean pair-end reads were aligned to the reference genome (hg38) using HISAT2, and the transcripts were merged by StringTie and Cuffmerge. Differential expression analysis was performed using the edgeR. Genes with  $P < 0.05$  and fold changes  $> 2$  were considered to be significantly differentially expressed. KOBAS software was used to evaluate the statistical enrichment Kyoto encyclopedia of genes and genomes (KEGG) pathways of differentially expressed genes.

## Real-Time PCR

Total RNA was isolated by using RNAiso Plus (TAKARA) following the instructions according to the manufacturers. Real-time PCR reactions were conducted using SYBR<sup>®</sup> Premix Ex Taq<sup>™</sup> II (TAKARA) on the 7500 Fast Real-Time PCR System (Applied Biosystems, Foster City, CA, United States) as previously described (Tan et al., 2017). The primer sequences are shown in **Table 1**. The relative mRNA levels were calculated by the comparative threshold method using glyceraldehyde-3-phosphate dehydrogenase (GAPDH) as an internal control for normalization.

## Generation and Infection of the Recombinant Adenoviral Vector

The coding region of Notch1 was amplified by RT-PCR and cloned into the adenoviral vector pHBAd-EF1-MCS-GFP by *in vitro* recombination. The empty vector served as an infection control. The recombinant plasmid was confirmed by DNA sequencing. The viral stocks were propagated in 293 cells. The cells were harvested 48 h after infection, and the concentrated virus was stored in aliquots at  $-80^{\circ}\text{C}$ . For adenoviral infection, TSCs were grown to 50–70% confluence and infected with either the Ad-notch1 adenovirus or the control adenovirus. After 48–72 h, TSCs were harvested for different analysis.

## Small Interfering RNA (siRNA) Synthesis and Transfection

siRNA specifically targeting Notch1 and control siRNA (scrambled) were designed and synthesized by GenePharma (Suzhou, China). The siRNA sequences were 5'-GCUGGA UACAAGUGCAACUTT-3' for Notch1 and 5'-UUCUCCG AACGUGUCACGUTT-3' for scrambled control. Transfections were carried out using Lipofectamine<sup>™</sup> RNAiMAX Transfection Reagent (Invitrogen) following the manufacturer's instructions. The transfected cells were harvested 48 or 72 h after transfection.

## Western Blot Analysis

Total proteins were extracted from cells using radioimmunoprecipitation assay (RIPA) lysis buffer (Beyotime

Institute of Biotechnology, Shanghai, China), and protein concentrations were measured by the bicinchoninic acid (BCA) assay. Equal amounts of proteins were boiled at  $100^{\circ}\text{C}$ , separated by sodium dodecyl sulfate polyacrylamide gel electrophoresis (SDS-PAGE), and transferred onto polyvinylidene fluoride (PVDF) membranes (Millipore, Bedford, MA, United States). Afterward, the membranes were blocked with 5% (w/v) skim milk at room temperature and immunoblotted overnight at  $4^{\circ}\text{C}$

**TABLE 1** | Sequences of primers used for real-time PCR.

Gene symbol		Sequence (5'-3')
PPAR $\gamma$	Forward	TTTCCGAAGAACCATCCGATT
	Reverse	ATGGCATTGTGAGACATCCCC
FABP4	Forward	TGAAATCACCGCAGACGACA
	Reverse	ACACATTCCACCACCAGCTT
Notch1	Forward	CCAGCAGATGATCTTCCCGTAC
	Reverse	TAGACAATGGAGCCACGGATGT
Notch2	Forward	ATGTGGACGAGTGTCTGTTGC
	Reverse	GGAAGCATAGGCACAGTCATC
Notch3	Forward	TGCCAGAGTTCAGTGGTGG
	Reverse	CACAGGCAAATCGGCCATC
Notch4	Forward	CTCTTGCCACTCAATTTCCCT
	Reverse	TTGCAGAGTTGGGTATCCCTG
DLL1	Forward	AGGGTGTGATGACCAACATGGA
	Reverse	TATCGGATGCACTCATCGCAGTA
DLL4	Forward	TTCCAGGCAACCTTCTCCGA
	Reverse	ACTGCCGCTATTCTTGTC
Jagged1	Forward	CCTCGGGTCAGTTTGAGCTG
	Reverse	CCTTGAGGCACACTTTGAAGTA
Jagged2	Forward	CAATGACACCACTCCAGATGAG
	Reverse	GGCCAAAGAAGTCGTTGCG
Hes1	Forward	GCAGACATTCTGAAATGACTGTGA
	Reverse	GAGTGCGCACCTCGGTGTTA
Hey1	Forward	CCGACGAGACCGAATCAATAAC
	Reverse	TCAGGTGATCCACAGTCATCTG
NRG1	Forward	GAGGTGAGAACACCCAAGTCA
	Reverse	TGGTCCCAGTCGTGGATGTAG
Impdh2	Forward	GATGGGGAGTCGATTGGTGG
	Reverse	GGTCTGTCCGGCAATGATG
USP47	Forward	GATGTGATTCCCTTGGATTGCT
	Reverse	AACCCCATTTGGTGTATCTTCTTC
MFF	Forward	ATGCCAGTGTGATAATGCAAGT
	Reverse	CTCGCTCTCTTCGCTTTG
CD36	Forward	ATGGGCTGTGATCGGAAGT
	Reverse	GTCTTCTCAATAAGCATGTCTCC
LPL	Forward	GGGAGTTTGGCTCCAGAGTTT
	Reverse	TGTGTCTTCAGGGTCCCTTAG
Plin1	Forward	GGGACCTGTGAGTGCTTCC
	Reverse	GTATTGAAGAGCCGGGATCTTTT
Adipoq	Forward	TGTTCTCTTAATCTGCCCA
	Reverse	CCAACCTGCACAAGTCCCTT
Fndc3b	Forward	GATGATGACCGACAGATCCC
	Reverse	GCTCTGATGGTAAAGGTCTCAC
GAPDH	Forward	TGTGTCCGTCGTGGATCTGA
	Reverse	TTGCTGTTGAAGTCGCAGGAG

with rabbit polyclonal antibody against LaminB (Wanleibio, Shenyang, China) and rabbit monoclonal antibody against LC3, Beclin1, AKT, mammalian target of rapamycin (mTOR), Notch1, p62 (all from Abcam, Cambridge, MA, United States), p-AKT, p-mTOR (both from Cell Signaling Technology, Danvers, MA, United States) and  $\beta$ -tubulin (Beyotime Institute of Biotechnology). Then, appropriate horseradish peroxidase (HRP)-conjugated secondary antibodies were applied, and the protein bands were detected by the enhanced chemiluminescence (ECL) detection system.  $\beta$ -tubulin and LaminB were used as a cytoplasm and nuclear loading control, respectively.

## Flow Cytometry

When reaching 80–90% confluence, cells were harvested and fixed with paraformaldehyde at room temperature for 1 h. Then,  $1 \times 10^6$  cells (100  $\mu$ l) were incubated with phycoerythrin (PE) labeled CD45 antibody (BioLegend, San Diego, CA, United States) at room temperature for 15 min in the dark. After

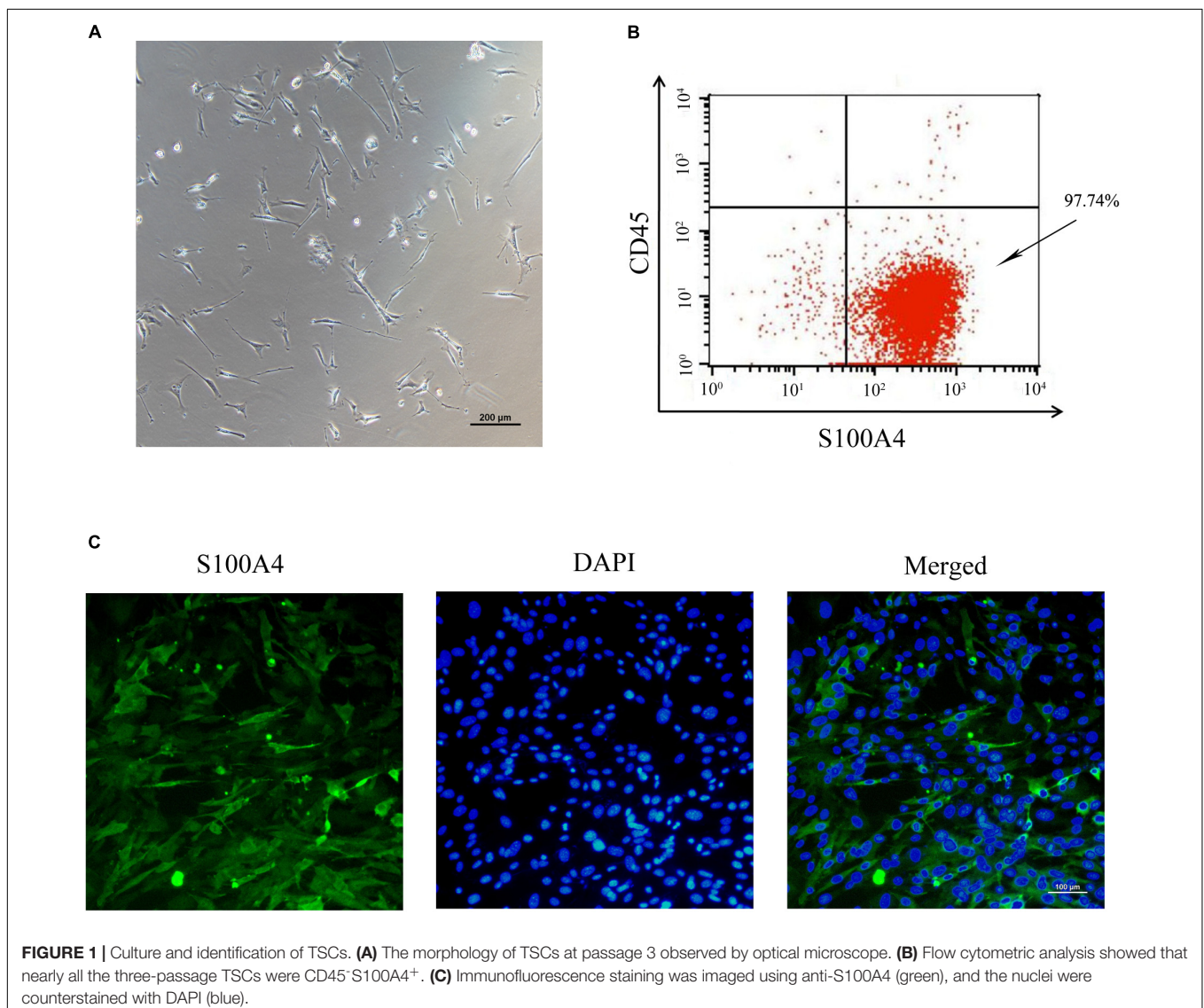
permeabilization with 0.5% Triton X-100, cells were incubated with a rabbit monoclonal S100A4 antibody (Abcam), followed by a corresponding Alexa Fluor<sup>®</sup> conjugated secondary antibody. Finally, the samples were analyzed with a FACSCalibur flow cytometer (BD Biosciences, Sunnyvale, CA, United States).

## Oil Red O Staining

The lipid accumulation in differentiated cells were visualized by Oil Red O staining using a commercially available kit (Leagene Biotechnology, Beijing, China) as previously reported (Tan et al., 2017).

## Quantification of Intracellular Lipids

The intracellular lipids in rosiglitazone-induced TSCs were quantified by using AdipoRed<sup>™</sup> reagent (Lonza, Walkersville, MD, United States) as previously described (Tan et al., 2017). After rosiglitazone treatment, AdipoRed<sup>™</sup> reagent was added into each well and incubated at room temperature for 10 min.



Fluorescence was measured on a plate reader with excitation set at 485 nm and emission at 572 nm.

## Immunofluorescence

Cells were grown on coverslips in 6-well plates, fixed in 4% paraformaldehyde at room temperature for 1 h, and permeabilized with 0.5% Triton X-100 in PBS for 20 min. After washing, unspecific binding sites were blocked with 5% FBS for 20 min at room temperature. Next, the coverslips were incubated overnight at 4°C with a rabbit monoclonal antibody against S100A4 (1:100 diluted, Abcam), followed by incubation with the fluorescein isothiocyanate (FITC)-labeled anti-rabbit IgG antibody. After stained the cell nuclei with 4', 6-diamidino-2-phenylindole (DAPI), the coverslips were observed under a fluorescence microscopy.

## Statistical Analysis

Raw data are shown as mean  $\pm$  standard deviation (SD). Statistical calculations were carried out using GraphPad Prism 5 (GraphPad Software, La Jolla, CA, United States). Differences among groups were analyzed by one-way analysis of variance (ANOVA) followed by the Bonferroni test for *post hoc* comparisons. A *P*-value less than 0.05 was considered to be statistically significant.

## RESULTS

### Culture and Adipogenic Differentiation of TSCs

To establish an *in vitro* primary TSC culture model, postnatal thymi were subjected to enzymatic digestion, and thymocytes were depleted during passaging. Upon culture for three passages, TSCs displayed fibroblast-like phenotype (**Figure 1A**). Flow cytometry analysis showed that nearly all TSCs expressed S100A4, but exhibited negligible expression of CD45 (**Figure 1B**). Furthermore, immunostaining showed that all TSCs were also

positive for S100A4, a fibroblast marker (**Figure 1C**). To induce adipogenic differentiation, TSCs were treated with PPAR $\gamma$  ligand rosiglitazone for 7 days, and Oil red O staining was performed to visualize lipid accumulation. Compared with DMSO-treated cells, intracellular lipid droplets were observed in TSCs treated with rosiglitazone (**Figure 2A**). In addition, real-time PCR analysis showed that the mRNA levels of adipogenic markers, PPAR $\gamma$  and fatty acid binding protein 4 (FABP4), were remarkably increased after rosiglitazone treatment (**Figure 2B**; *P* < 0.01). Therefore, we successfully cultured primary TSCs, which offer us a useful cellular model to investigate the mechanisms underlying thymic adipogenesis.

### Identification of Differentially Expressed Genes During Adipogenic Transformation in TSCs by RNA-Seq

In order to identify key regulators in thymic adipogenesis, RNA-seq analysis was carried out in DMSO- and rosiglitazone-treated TSCs. As a result, we identified a total of 1737 genes differed significantly at *P* < 0.05 with a fold change > 2, among which 965 genes were up-regulated and 772 genes were down-regulated in rosiglitazone-treated cells compared with DMSO-treated cells. The complete list of these genes is shown in **Supplementary Table S1**. The differentially expressed genes are also represented in a volcano plot (**Figure 3A**). Unsupervised hierarchical clustering analysis revealed that DMSO-treated cells are distinctly different from rosiglitazone-treated cells (**Figure 3B**). In order to identify the potential functions of these differentially expressed genes, we performed gene ontology (GO) enrichment analysis and found that the GO terms were enriched in metabolic process, intracellular, and protein binding (**Supplementary Table S2**). KEGG analysis was carried out to assess the involved pathways of the differentially expressed genes. The results showed that a number of pathways, including ubiquitin mediated proteolysis, PPAR signaling pathway, and mTOR signaling pathway were

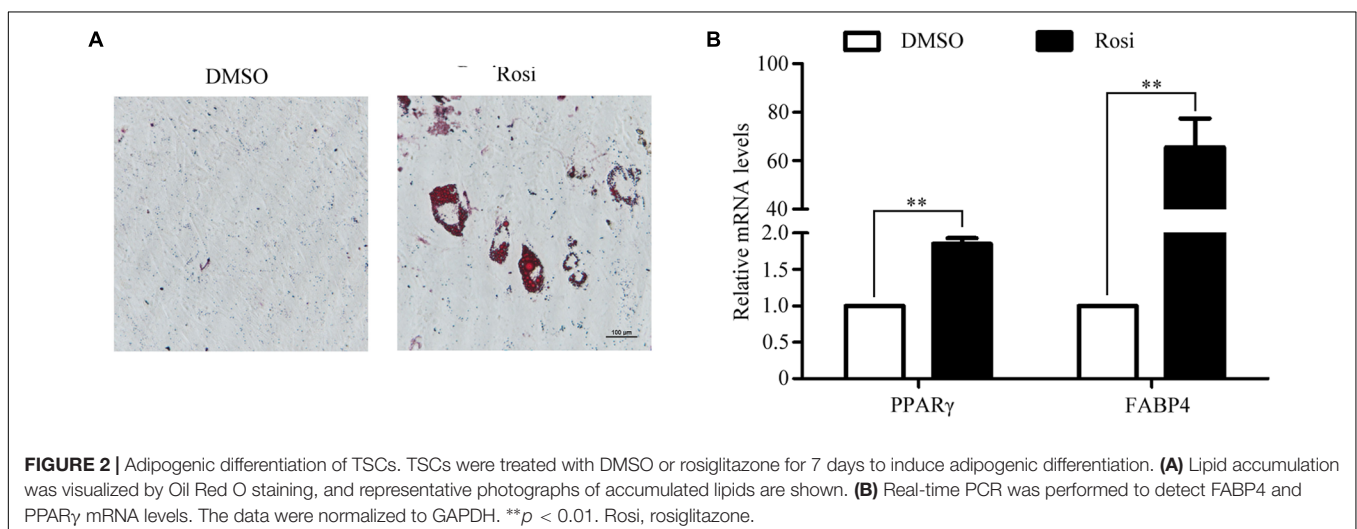
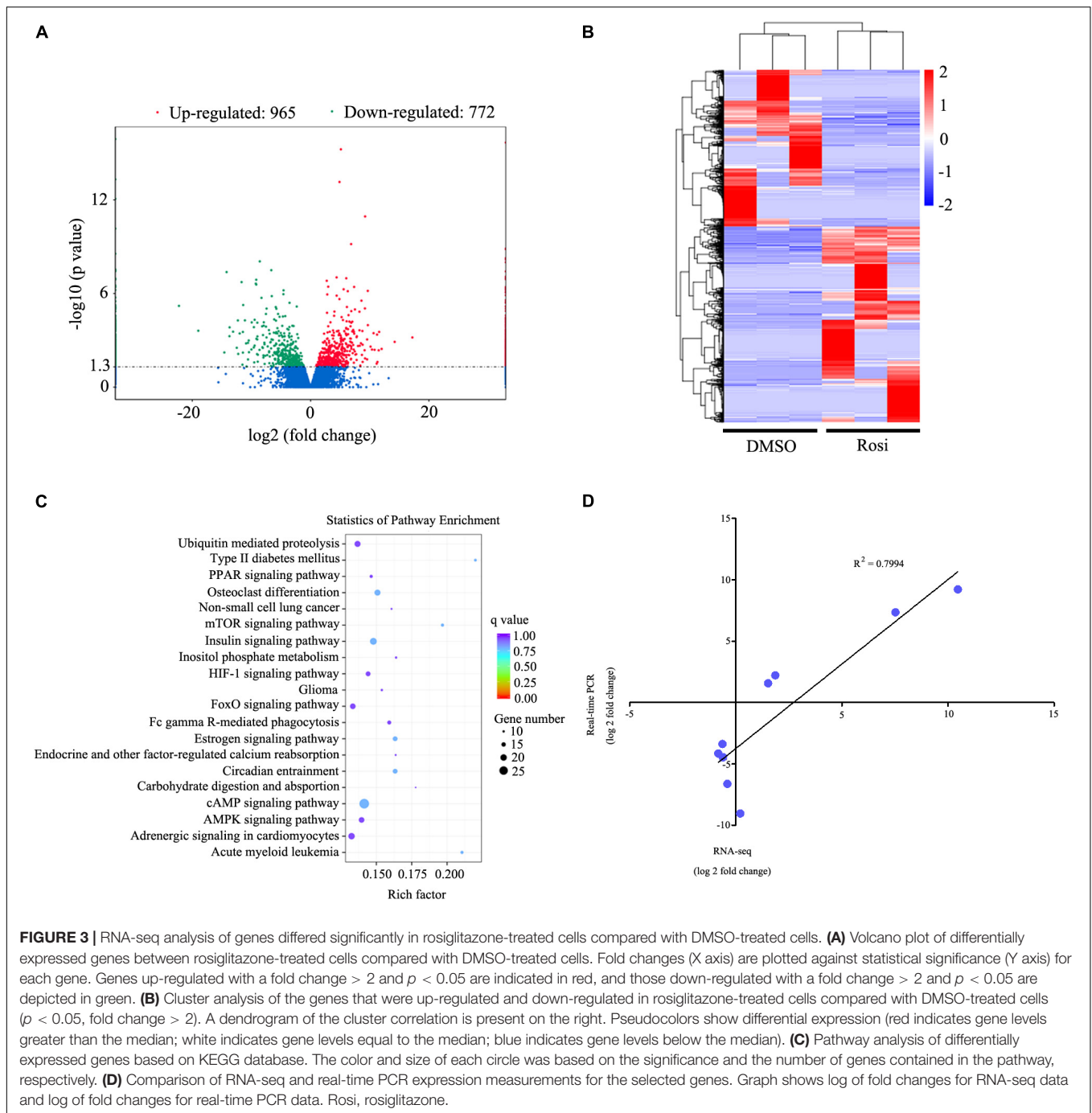


**FIGURE 2 |** Adipogenic differentiation of TSCs. TSCs were treated with DMSO or rosiglitazone for 7 days to induce adipogenic differentiation. **(A)** Lipid accumulation was visualized by Oil Red O staining, and representative photographs of accumulated lipids are shown. **(B)** Real-time PCR was performed to detect FABP4 and PPAR $\gamma$  mRNA levels. The data were normalized to GAPDH. \*\**p* < 0.01. Rosi, rosiglitazone.



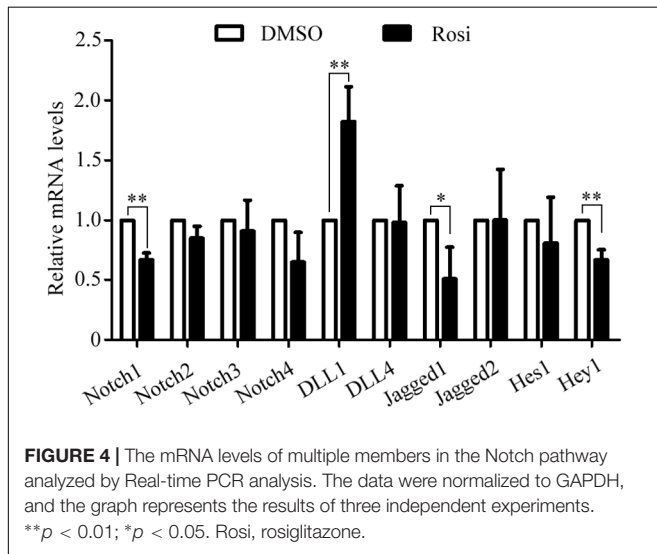
predominantly over-represented (Figure 3C;  $P < 0.05$ ). To validate the results of RNA-seq analysis, real-time PCR was conducted to detect a number of candidate genes (Table 1). Fold-change differences detected by real-time PCR were not as pronounced as those observed in RNA-seq analysis. However, when the log of the fold change in gene expression as determined by real-time PCR was plotted against the log of the fold change as determined by RNA-seq analysis, there was a clear correlation between the two methods ( $R^2 = 0.7994$ ; Figure 3D). These data indicate that the results observed

by real-time PCR were consistent with those of RNA-seq analysis.

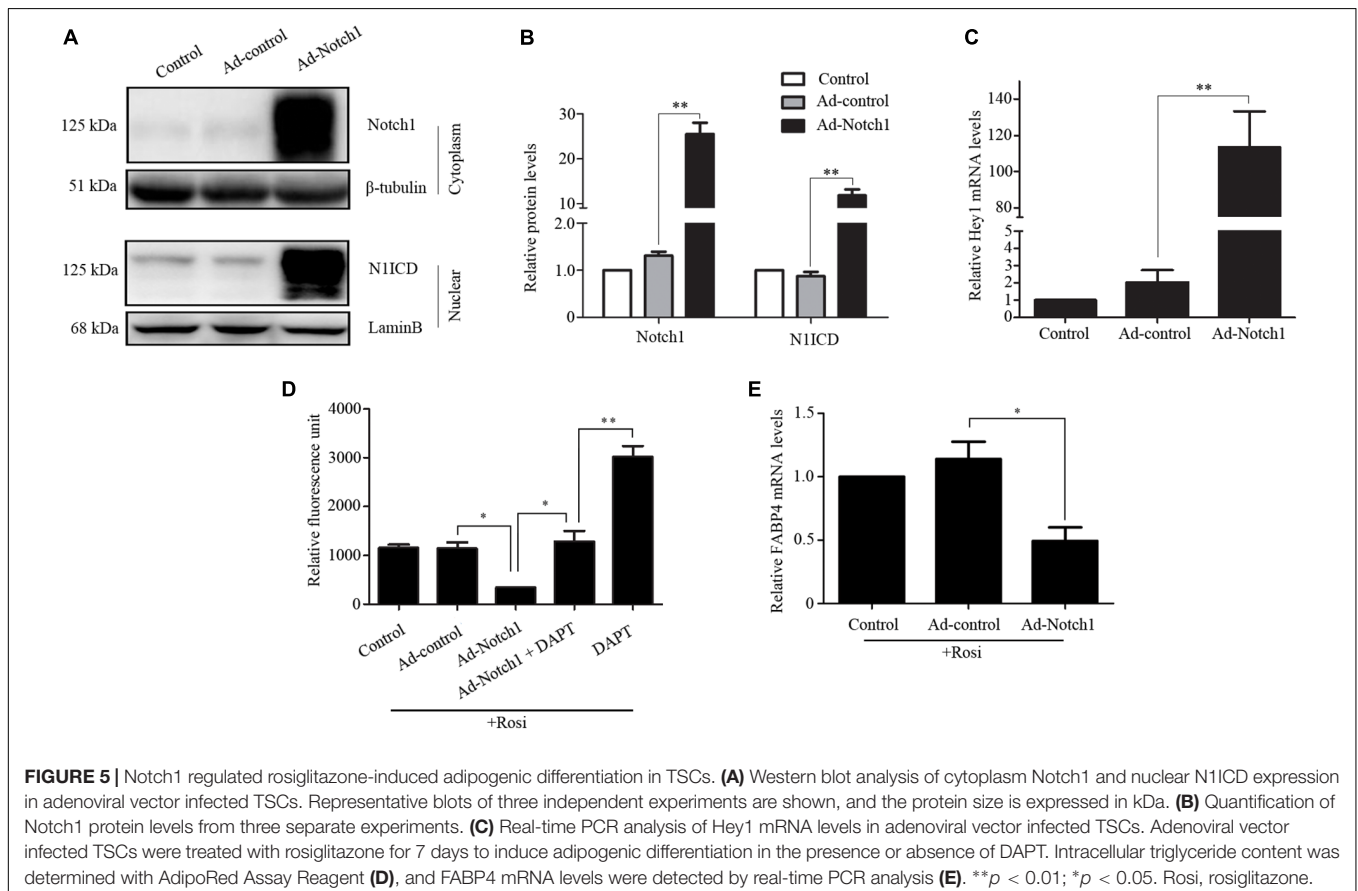
### Overexpression of Notch1 Attenuated and Inhibition of Notch1 Promoted Rosiglitazone-Induced Adipogenic Differentiation in TSCs

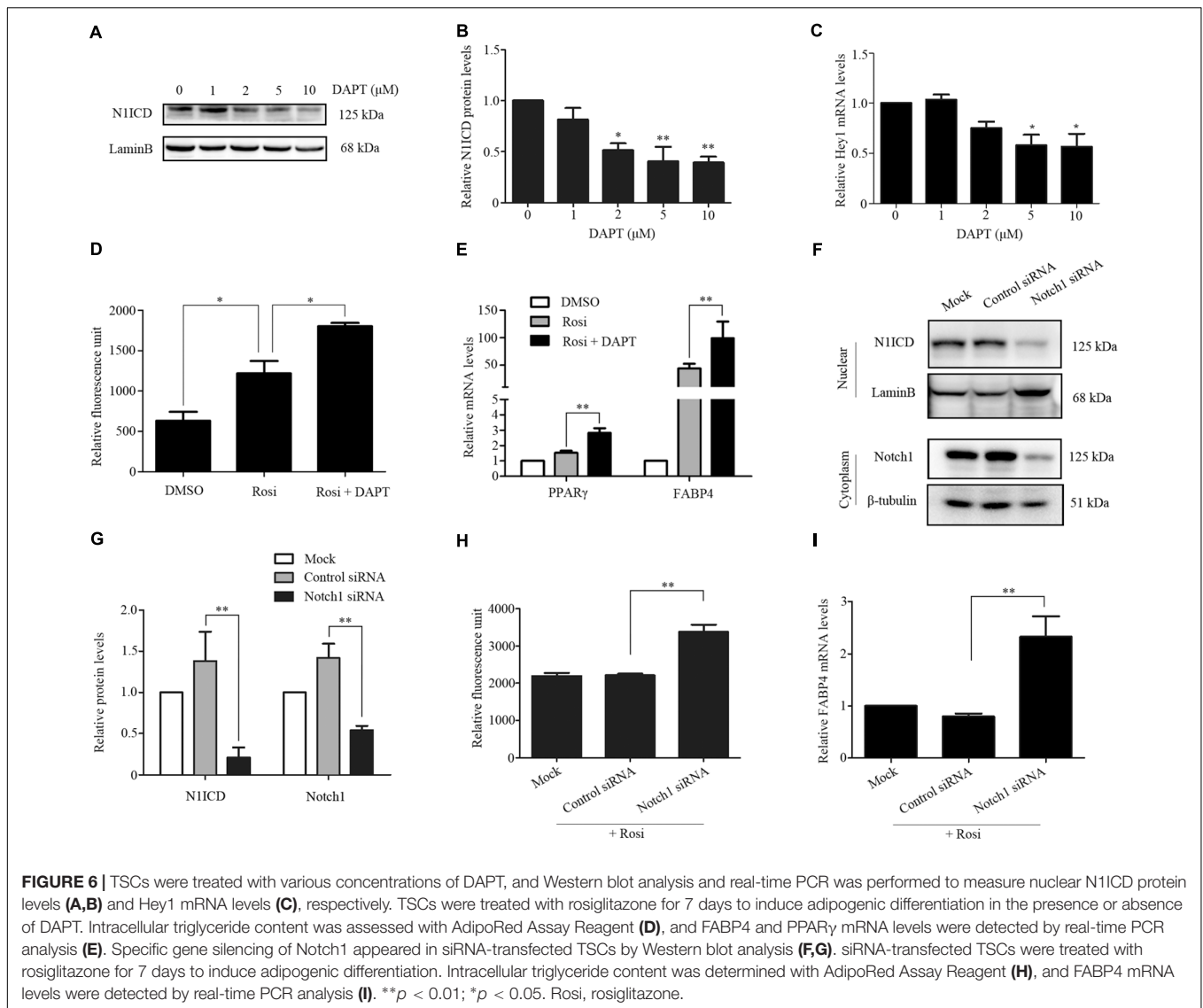
We note that several members of the Notch pathway were significantly altered in RNA-seq analysis. Therefore, real-time

PCR was carried out to evaluate the expression of multiple members in the Notch pathway. We found that Notch1, Jagged1 and Hey1 were significantly down-regulated, while DLL1 was dramatically up-regulated in rosiglitazone-treated TSCs compared to control TSCs (Figure 4), suggesting a potential role of the Notch pathway in thymic adipogenesis. Next, the



adenoviral vector carrying Notch1 gene was constructed and transduced into TSCs. Substantial increases in Notch1 protein levels, N1ICD nuclear translocation (Figures 5A,B;  $P < 0.01$ ), and Hey1 mRNA levels (Figure 5C;  $P < 0.01$ ) were observed in TSCs infected with adenoviral vector carrying Notch1 gene in comparison to control cells, suggesting activation of Notch pathway. Moreover, the effects of Notch1 on adipogenic differentiation were investigated by measuring the intracellular triglyceride content with a commercially available AdipoRed Assay Reagent. We found that overexpression of Notch1 inhibited rosiglitazone-induced increases in intracellular triglyceride content (Figure 5D) and FABP4 mRNA levels (Figure 5E) in TSCs. In contrast, DAPT, an inhibitor of Notch signaling, potentially attenuated the inhibitory effects of Notch1 overexpression on adipogenic differentiation (Figure 5D). Furthermore, DAPT down-regulated the nuclear expression of N1ICD protein (Figures 6A,B) and Hey1 mRNA levels (Figure 6C) in a dose-dependent manner. DAPT also substantially promoted rosiglitazone-induced increases in intracellular triglyceride content (Figure 6D) and PPAR $\gamma$  and FABP4 mRNA levels (Figure 6E). To further characterize the role of Notch1 in adipogenic differentiation of TSCs, we employed an RNA interference approach to knockdown Notch1 expression in TSCs and found that both cytoplasm Notch1 and nuclear N1ICD protein levels in cells transfected with specific siRNA for Notch1 were significantly reduced compared with





those transfected with control siRNA (Figures 6F,G). Similar to DAPT, knockdown of Notch1 also dramatically promoted rosiglitazone-induced increases in intracellular triglyceride content (Figure 6H) and FABP4 mRNA levels (Figure 6I). Taken together, these findings demonstrate that Notch1 negatively regulates rosiglitazone-induced adipogenic differentiation in TSCs.

### DAPT, an Inhibitor of Notch Signaling, Induced Autophagy and Adipogenic Differentiation in TSCs via Inhibition of AKT/mTOR Pathway

Autophagy is known to be a degradation process of intracellular proteins and organelles during adipogenesis (Goldman et al., 2011; Zhang et al., 2012; Ahmed et al., 2018). To investigate the role of autophagy in adipogenic differentiation in TSCs, the expression levels of several autophagy markers,

including LC3, Beclin1, and p62 during adipogenesis were determined by Western blot analysis. As illustrated in Figure 7, p62 was down-regulated from day 3 onward, suggesting activation of autophagy during adipogenesis. However, the levels of LC3-II/I and Beclin1 remained unchanged during adipogenesis (Figure 7). To evaluate the effects of Notch signaling on autophagy, TSCs were treated with various concentrations of DAPT for 48 h. We found that DAPT dose-dependently increased the ratio of LC3-II/LC3-I, but reduced the protein levels of p62 in TSCs (Figure 8). Meanwhile, DAPT also decreased the levels p-AKT and p-mTOR in a dose-dependent fashion (Figure 8). To test whether DAPT-induced adipogenesis is dependent on autophagy activation, TSCs were incubated with autophagy inhibitor 3-MA (5 mM) in the absence or presence of DAPT during adipogenesis. Adipogenesis was determined by measuring intracellular triglyceride content and mRNA levels of PPAR $\gamma$  and FABP4. We found that

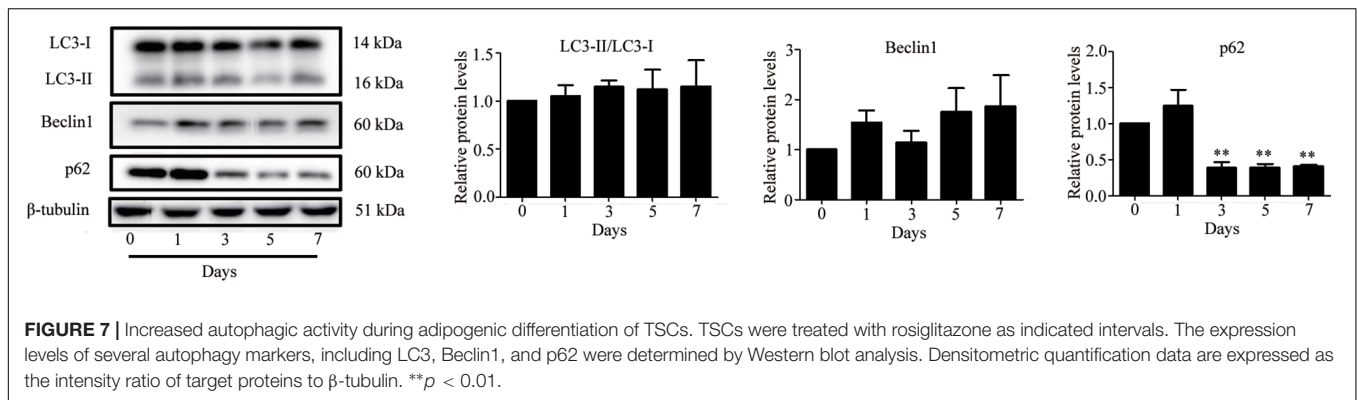


**FIGURE 7 |** Increased autophagic activity during adipogenic differentiation of TSCs. TSCs were treated with rosiglitazone as indicated intervals. The expression levels of several autophagy markers, including LC3, Beclin1, and p62 were determined by Western blot analysis. Densitometric quantification data are expressed as the intensity ratio of target proteins to  $\beta$ -tubulin. \*\* $p < 0.01$ .

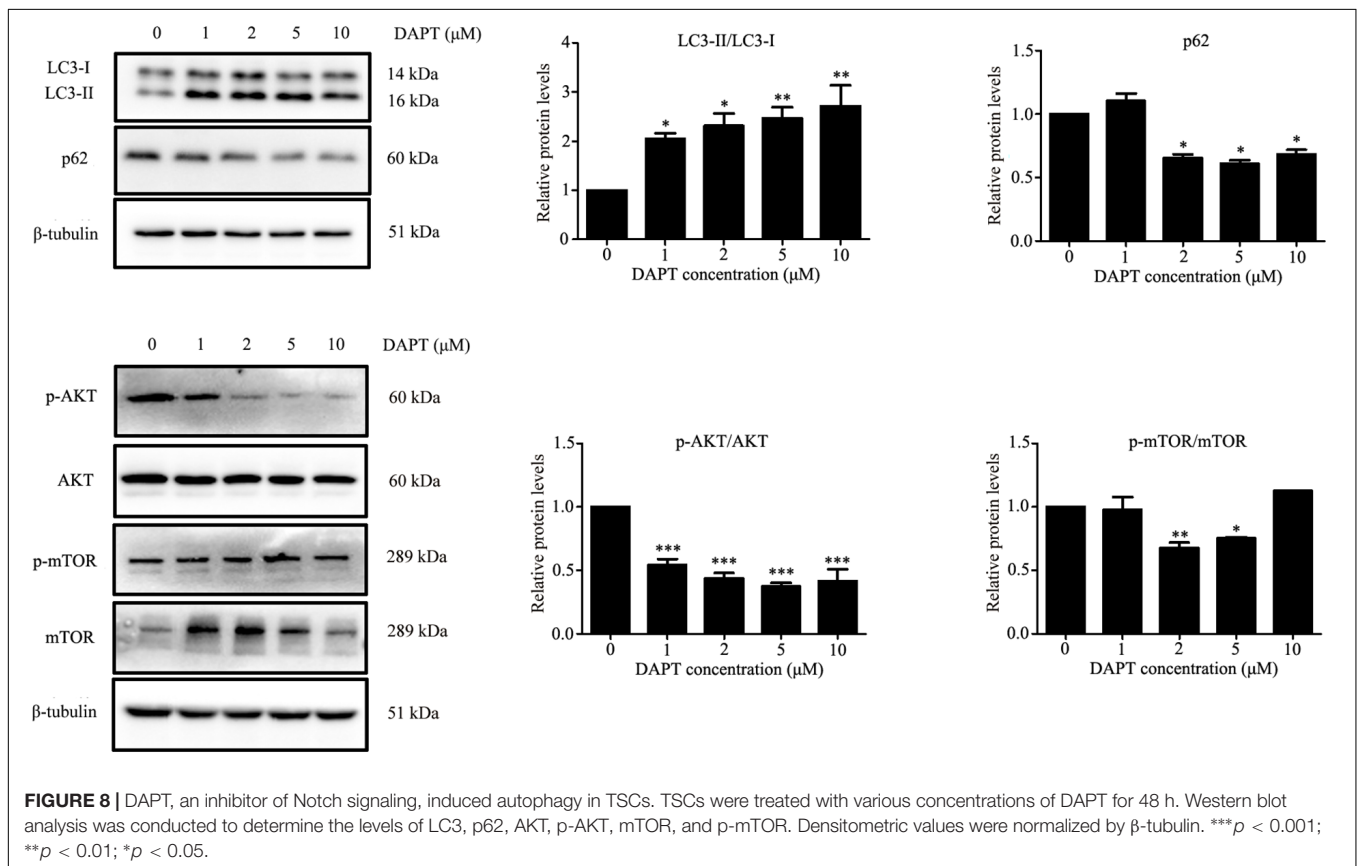


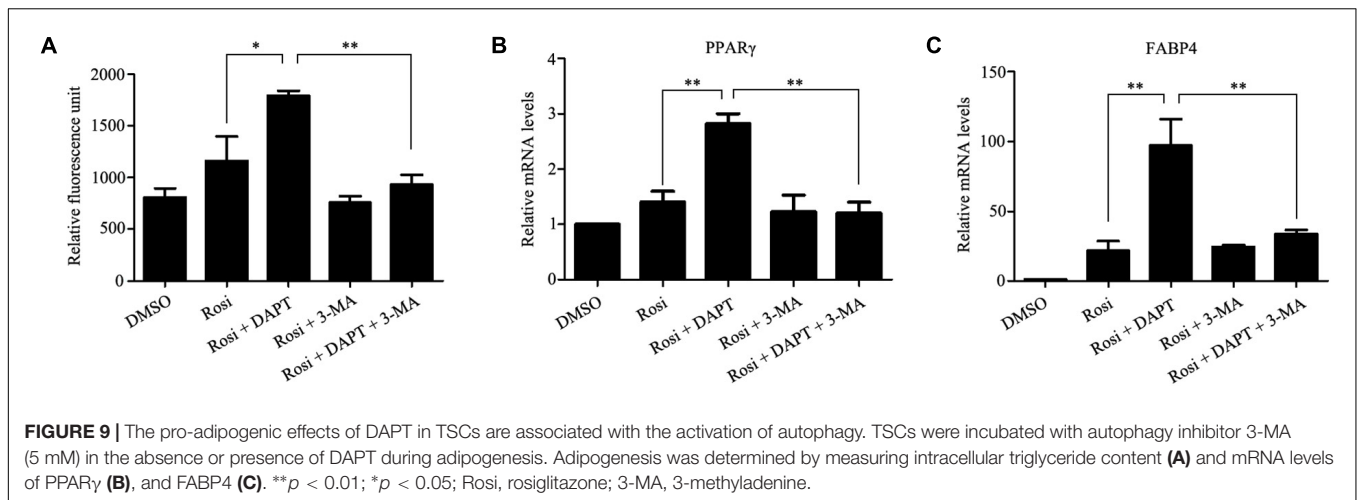
**FIGURE 8 |** DAPT, an inhibitor of Notch signaling, induced autophagy in TSCs. TSCs were treated with various concentrations of DAPT for 48 h. Western blot analysis was conducted to determine the levels of LC3, p62, AKT, p-AKT, mTOR, and p-mTOR. Densitometric values were normalized by  $\beta$ -tubulin. \*\*\* $p < 0.001$ ; \*\* $p < 0.01$ ; \* $p < 0.05$ .

3-MA abolished the pro-adipogenic effects of DAPT in TSCs (Figures 9A–C), suggesting that the pro-adipogenic effects of DAPT in TSCs are associated with the activation of autophagy. Collectively, our results reveal that Notch1 inhibits rosiglitazone-induced adipogenic differentiation in TSCs (Figure 10).

## DISCUSSION

In the present study, we successfully cultured primary TSCs and performed a comprehensive analysis of differentially expressed genes during adipogenesis of TSCs by using

RNA-seq method. As a result, we identified a total of 1737 differentially expressed genes, among which 965 genes were up-regulated and 772 genes were down-regulated in rosiglitazone-treated cells compared with DMSO-treated cells. GO enrichment analysis showed that the GO terms were enriched in metabolic process, intracellular, and protein binding. KEGG analysis showed that a number of pathways, including ubiquitin mediated proteolysis, PPAR signaling pathway, and mTOR signaling pathway were predominantly over-represented. Our further experiments demonstrated that overexpression of Notch1 suppressed, while the Notch signaling inhibitor DAPT promoted adipogenic differentiation in TSCs, and the pro-adipogenic effects of



DAPT were associated with the activation of autophagy. Taken together, our results suggest that Notch1 is a key regulator in thymic adipogenesis and may serve as a potential target to hinder thymic adiposity in age-related thymic involution.

The thymus is constituted by a myriad of cell types, such as thymocyte, macrophages, fibroblasts, dendritic cells, and epithelial cells (Xing and Hogquist, 2014; Tan J.X. et al., 2016). In the present study, postnatal thymi were subjected to enzymatic digestion, and suspension cells were cultured. Upon culture, approximately 97.74% cells were CD45<sup>-</sup>S100A4<sup>+</sup> and exhibited fibroblast-like phenotype. This is largely due to the fact that thymocytes are removed by refreshing the medium, and fibroblasts proliferate at a faster rate than other cells. Our results are consistent with the findings by Yang et al. (2009). This culture system offers us a useful cellular model to investigate the mechanisms underlying thymic adipogenesis.

Age-related thymic involution is accompanied by loss of thymic epithelial cell (TECs) and increase in fibroblasts (Gray et al., 2007; Aw et al., 2008). Several lines of evidence demonstrate that fibroblasts can be readily induced to develop into adipocytes and represent a cellular source of thymic adipogenesis (Youm et al., 2009; Tan J. et al., 2016; Sheridan et al., 2017). The nuclear receptor PPAR $\gamma$  has been shown to maintain insulin sensitivity and stimulate adipogenesis (Oger et al., 2014). PPAR $\gamma$  plays a key role in white adipose tissue differentiation, and forced PPAR $\gamma$  expression in nonadipogenic cells leads to their adipocyte differentiation (Evans et al., 2004; Rosen and MacDougald, 2006). Furthermore, Yang et al. (2009) have reported high PPAR $\gamma$  protein levels in aging thymus, suggesting PPAR $\gamma$ -driven adipogenesis of thymic fibroblasts. Rosiglitazone, a PPAR $\gamma$  ligand, has been commonly used to induce transdifferentiation of multipotential cells into adipocytes, such as proadipocytes (Kim et al., 2016), bone marrow-derived mesenchymal stem cells (Lu et al., 2016), and embryonic stem cells (Xiong

et al., 2005). We and other have also used rosiglitazone to induce adipocyte differentiation of OP9-DL1 cells (Tan et al., 2017) and primary TSCs (Yang et al., 2009). In the present study, we performed a comprehensive analysis of differentially expressed genes during adipogenesis of TSCs by using RNA-seq method and identified a total of 1737 differentially expressed genes. GO enrichment analysis showed that the GO terms were enriched in metabolic process, intracellular, and protein binding. KEGG analysis showed that a number of pathways, including ubiquitin mediated proteolysis, PPAR signaling pathway, and mTOR signaling pathway were predominantly over-represented. However, further investigations are needed to uncover the functions of these altered genes in adipocyte differentiation of TSCs.

The Notch signaling pathway is a highly conserved signaling pathway that regulates cell proliferation, cell fate, differentiation, and cell death (Yamamoto et al., 2014). Currently, the function of Notch signaling pathway in adipocyte differentiation remains controversial (Shan et al., 2017). Activation of Notch signaling inhibits the differentiation of 3T3-L1 cells by regulating the target gene *Hes1* (Ross et al., 2004). Mechanically, *Hes1* can directly repress expression of *C/EBP $\alpha$*  and PPAR $\gamma$  (Ross et al., 2006). Song et al have documented that inhibition of Notch signaling promotes adipogenic differentiation of mesenchymal stem cells (Song et al., 2015). Nonetheless, inhibition of Notch signaling by soluble Jagged1 blocks the differentiation of 3T3-L1 preadipocytes (Ross et al., 2004). In the present study, we note that several members of Notch pathways were significantly altered in RNA-seq analysis. Therefore, real-time PCR was carried out to evaluate the expression of multiple members in the Notch pathway. We found that *Notch1*, *Jagged1* and *Hey1* were significantly down-regulated, while *DLL1* was dramatically up-regulated in rosiglitazone-treated TSCs compared to control TSCs, suggesting a potential role of the Notch pathway in thymic adipogenesis. Our further experiments showed that overexpression of *Notch1*

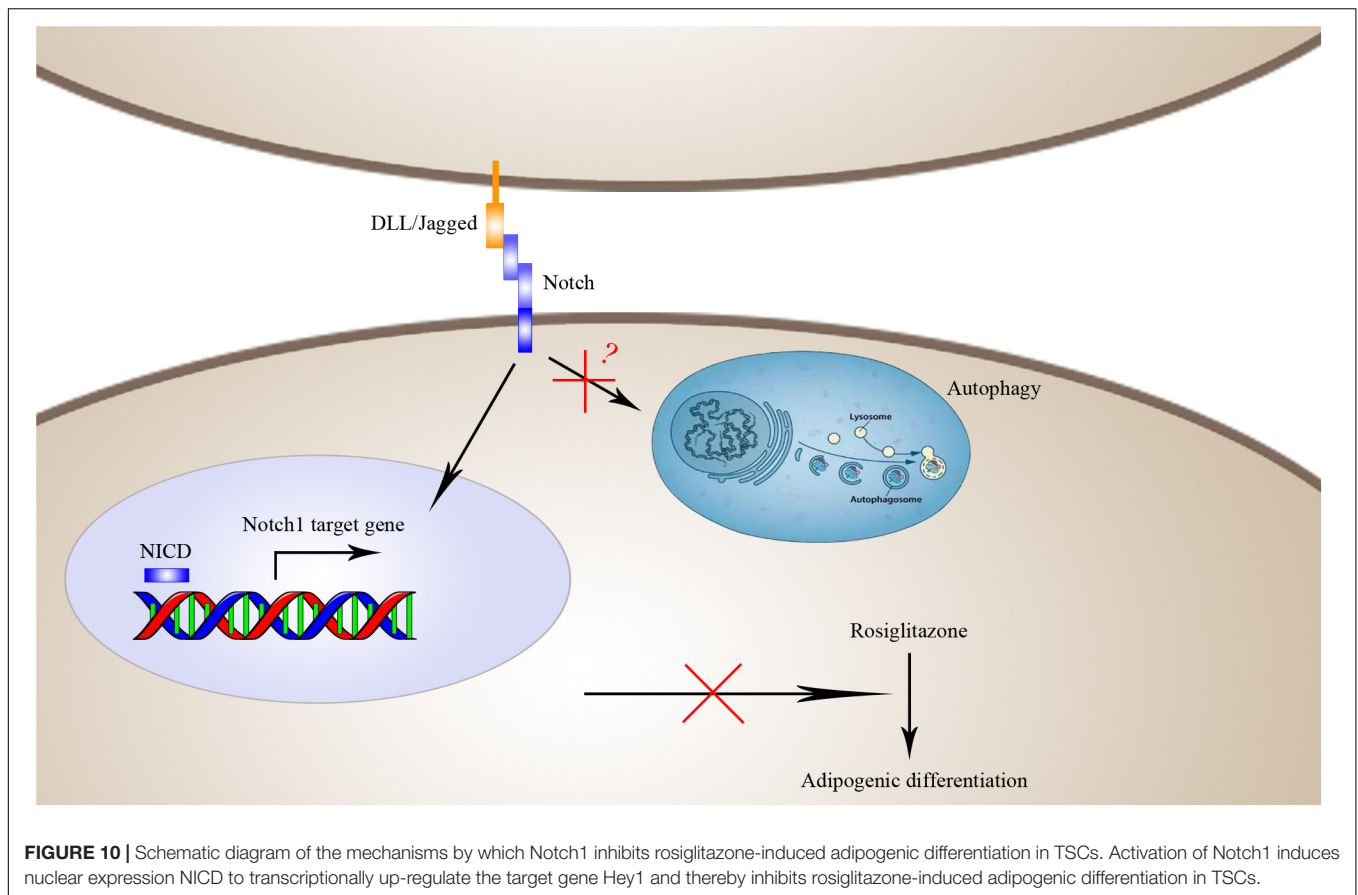


**FIGURE 10** | Schematic diagram of the mechanisms by which Notch1 inhibits rosiglitazone-induced adipogenic differentiation in TSCs. Activation of Notch1 induces nuclear expression NICD to transcriptionally up-regulate the target gene Hey1 and thereby inhibits rosiglitazone-induced adipogenic differentiation in TSCs.

inhibited, and DAPT, an inhibitor of Notch signaling, and knockdown of Notch1 promoted rosiglitazone-induced adipogenic differentiation in TSCs. Consequently, our data support a negative role of Notch signaling in adipogenic differentiation of TSCs. However, Aw and co-workers found increased expression of Notch1 in the thymi of older mice using immunohistochemistry (Aw et al., 2009). This conflict could be explained by the fact that upregulation of Notch1 with increasing age, amongst the TEC populations, is mostly confined to those within the cortex, and other cell types, including thymocytes may contribute to the rise in Notch1 expression in older mice (Aw et al., 2009). Thus, it is essential to analyze the expression of Notch1 in specific thymic cell populations.

Recent evidence suggests a pivotal role of autophagy in adipocyte differentiation (Tao et al., 2017), and increased autophagy in adipose tissues has been observed in obese humans and animals (Kovsan et al., 2011; Jansen et al., 2012; Nunez et al., 2013). In this study, we consistently found increased autophagy in adipogenic differentiation of TSCs, as evidence by reduced expression of p62. To further clarify the mechanisms by which Notch signaling pathway mediates adipogenic differentiation of TSCs, the effects of DAPT on LC3, p62, and AKT/mTOR were determined by Western blot analysis. We found that DAPT increased the ratio of LC3-II/LC3-I, but reduced the protein levels of

p62, p-AKT and p-mTOR in TSCs, suggesting increased autophagy. Additionally, we demonstrated that 3-MA, an autophagy inhibitor abolished the pro-adipogenic effects of DAPT in TSCs, suggesting that the pro-adipogenic effects of DAPT in TSCs were associated with the activation of autophagy. These results are largely in agreement with results by Song et al in mesenchymal stem cells (Song et al., 2015). Moreover, the autophagic process is essential for the presentation of self-Ags in the thymus to shape the T-cell repertoires (Kasai et al., 2009), and TECs possess a high constitutive level of autophagy, which is decreased with advancing of age (Uddin et al., 2012). However, the autophagic activity in thymic fibroblasts at different ages needs to be further investigated.

## CONCLUSION

In conclusion, our RNA-seq analysis identified a number of differentially expressed genes and associated signaling pathways in the adipocyte differentiation of primary TSCs. Moreover, we demonstrated that Notch1 inhibits rosiglitazone-induced adipogenic differentiation in TSCs, and increased autophagy was observed in rosiglitazone-induced adipogenic differentiation in TSCs. Our findings not only offer the basis for identification

of key mediators in thymic adipogenesis, but also uncover a negative role of Notch1 in thymic adiposity. Activation of Notch1 pathway may be an effective strategy to inhibit thymic adiposity in age-related thymic involution.

## AUTHOR CONTRIBUTIONS

YW, JT, and XZ conceived and designed the experiments. YW, JT, HD, and XL performed the experiments. HD and SilW analyzed the data. YW, JT, SimW, and ZY contributed reagents, materials, analysis tools. YW and XZ wrote the paper.

## REFERENCES

- Ahmed, M., Hwang, J. S., Lai, T. H., Zada, S., Nguyen, H. Q., Pham, T. M., et al. (2018). Co-Expression network analysis of AMPK and autophagy gene products during adipocyte differentiation. *Int. J. Mol. Sci.* 19:E1808. doi: 10.3390/ijms19061808
- Aw, D., and Palmer, D. B. (2011). The origin and implication of thymic involution. *Aging Dis.* 2, 437–443.
- Aw, D., Silva, A. B., Maddick, M., von Zglinicki, T., and Palmer, D. B. (2008). Architectural changes in the thymus of aging mice. *Aging Cell* 7, 158–167. doi: 10.1111/j.1474-9726.2007.00365.x
- Aw, D., Taylor-Brown, F., Cooper, K., and Palmer, D. B. (2009). Phenotypical and morphological changes in the thymic microenvironment from ageing mice. *Biogerontology* 10, 311–322. doi: 10.1007/s10522-008-9182-2
- Chaudhry, M. S., Velardi, E., Dudakov, J. A., and van den Brink, M. R. (2016). Thymus: the next (re)generation. *Immunol. Rev.* 271, 56–71. doi: 10.1111/immr.12418
- Ernszt, D., Banfai, K., Kellermayer, Z., Pap, A., Lord, J. M., Pongracz, J. E., et al. (2017). PPARgamma deficiency counteracts thymic senescence. *Front. Immunol.* 8:1515. doi: 10.3389/fimmu.2017.01515
- Evans, R. M., Barish, G. D., and Wang, Y. X. (2004). PPARs and the complex journey to obesity. *Nat. Med.* 10, 355–361. doi: 10.1038/nm1025
- Flores, K. G., Li, J., Sempowski, G. D., Haynes, B. F., and Hale, L. P. (1999). Analysis of the human thymic perivascular space during aging. *J. Clin. Invest.* 104, 1031–1039. doi: 10.1172/JCI7558
- Goldman, S. J., Zhang, Y., and Jin, S. (2011). Autophagic degradation of mitochondria in white adipose tissue differentiation. *Antioxid. Redox. Signal.* 14, 1971–1978. doi: 10.1089/ars.2010.3777
- Gray, D. H., Tull, D., Ueno, T., Seach, N., Classon, B. J., Chidgey, A., et al. (2007). A unique thymic fibroblast population revealed by the monoclonal antibody MTS-15. *J. Immunol.* 178, 4956–4965. doi: 10.4049/jimmunol.178.8.4956
- Gui, J., Mustachio, L. M., Su, D. M., and Craig, R. W. (2012). Thymus size and age-related thymic involution: early programming, sexual dimorphism, progenitors and stroma. *Aging Dis.* 3, 280–290.
- Jansen, H. J., van Essen, P., Koenen, T., Joosten, L. A., Netea, M. G., Tack, C. J., et al. (2012). Autophagy activity is up-regulated in adipose tissue of obese individuals and modulates proinflammatory cytokine expression. *Endocrinology* 153, 5866–5874. doi: 10.1210/en.2012-1625
- Kasai, M., Tanida, I., Ueno, T., Kominami, E., Seki, S., Ikeda, T., et al. (2009). Autophagic compartments gain access to the MHC class II compartments in thymic epithelium. *J. Immunol.* 183, 7278–7285. doi: 10.4049/jimmunol.0804087
- Kim, J., Lee, Y. J., Kim, J. M., Lee, S. Y., Bae, M. A., Ahn, J. H., et al. (2016). PPARgamma agonists induce adipocyte differentiation by modulating the expression of Lipin-1, which acts as a PPARgamma phosphatase. *Int. J. Biochem. Cell Biol.* 81(Pt A), 57–66. doi: 10.1016/j.biocel.2016.10.018
- Kovsan, J., Blucher, M., Tarnowski, T., Kloting, N., Kirshtein, B., Madar, L., et al. (2011). Altered autophagy in human adipose tissues in obesity. *J. Clin. Endocrinol. Metab.* 96, E268–E277. doi: 10.1210/jc.2010-1681

## FUNDING

This study was supported by a grant from the National Natural Science Foundation of China (No. 81801373).

## SUPPLEMENTARY MATERIAL

The Supplementary Material for this article can be found online at: <https://www.frontiersin.org/articles/10.3389/fphar.2018.01284/full#supplementary-material>

**TABLE S1** | The complete list of differentially expressed genes.

**TABLE S2** | Enriched GO terms of differentially expressed genes.

- Lu, W., Wang, W., Wang, S., Feng, Y., and Liu, K. (2016). Rosiglitazone promotes bone marrow adipogenesis to impair myelopoiesis under stress. *PLoS One* 11:e0149543. doi: 10.1371/journal.pone.0149543
- McGettigan, P. A. (2013). Transcriptomics in the RNA-seq era. *Curr. Opin. Chem. Biol.* 17, 4–11. doi: 10.1016/j.cbpa.2012.12.008
- Nunez, C. E., Rodrigues, V. S., Gomes, F. S., Moura, R. F., Victorio, S. C., Bombassaro, B., et al. (2013). Defective regulation of adipose tissue autophagy in obesity. *Int. J. Obes.* 37, 1473–1480. doi: 10.1038/ijo.2013.27
- Oger, F., Dubois-Chevalier, J., Gheeraert, C., Avner, S., Durand, E., Froguel, P., et al. (2014). Peroxisome proliferator-activated receptor gamma regulates genes involved in insulin/insulin-like growth factor signaling and lipid metabolism during adipogenesis through functionally distinct enhancer classes. *J. Biol. Chem.* 289, 708–722. doi: 10.1074/jbc.M113.526996
- Rosen, E. D., and MacDougald, O. A. (2006). Adipocyte differentiation from the inside out. *Nat. Rev. Mol. Cell Biol.* 7, 885–896. doi: 10.1038/nrm2066
- Ross, D. A., Hannenhalli, S., Tobias, J. W., Cooch, N., Shiekhatter, R., and Kadesch, T. (2006). Functional analysis of Hes-1 in preadipocytes. *Mol. Endocrinol.* 20, 698–705. doi: 10.1210/me.2005-0325
- Ross, D. A., Rao, P. K., and Kadesch, T. (2004). Dual roles for the Notch target gene Hes-1 in the differentiation of 3T3-L1 preadipocytes. *Mol. Cell. Biol.* 24, 3505–3513. doi: 10.1128/MCB.24.8.3505-3513.2004
- Shan, T., Liu, J., Wu, W., Xu, Z., and Wang, Y. (2017). Roles of notch signaling in adipocyte progenitor cells and mature adipocytes. *J. Cell. Physiol.* 232, 1258–1261. doi: 10.1002/jcp.25697
- Sheridan, J. M., Keown, A., Policheni, A., Roesley, S. N. A., Rivlin, N., Kadouri, N., et al. (2017). Thymospheres are formed by mesenchymal cells with the potential to generate adipocytes, but not epithelial cells. *Cell Rep.* 21, 934–942. doi: 10.1016/j.celrep.2017.09.090
- Song, B. Q., Chi, Y., Li, X., Du, W. J., Han, Z. B., Tian, J. J., et al. (2015). Inhibition of notch signaling promotes the adipogenic differentiation of mesenchymal stem cells through autophagy activation and PTEN-PI3K/AKT/mTOR Pathway. *Cell Physiol. Biochem.* 36, 1991–2002. doi: 10.1159/000430167
- Tan, J., Wang, Y., Wang, S., Zhang, N., Wu, S., Yuan, Z., et al. (2017). Untargeted metabolomics analysis of adipogenic transformation in OP9-DL1 cells using liquid chromatography-mass spectrometry: implications for thymic adipogenesis. *Cell Biol. Int.* 41, 447–456. doi: 10.1002/cbin.10740
- Tan, J., Wang, Y., Zhang, N., and Zhu, X. (2016). Induction of epithelial to mesenchymal transition (EMT) and inhibition on adipogenesis: two different sides of the same coin? Feasible roles and mechanisms of transforming growth factor beta1 (TGF-beta1) in age-related thymic involution. *Cell Biol. Int.* 40, 842–846. doi: 10.1002/cbin.10625
- Tan, J. X., Wang, Y. J., and Zhu, X. K. (2016). [Progresses in therapeutic strategies for thymic rejuvenation]. *Sheng Li Xue Bao* 68, 75–86.
- Tao, Z., Liu, L., Zheng, L. D., and Cheng, Z. (2017). Autophagy in adipocyte differentiation. *Methods Mol. Biol.* 1854, 45–53. doi: 10.1007/7651\_2017\_65
- Uddin, M. N., Nishio, N., Ito, S., Suzuki, H., and Isobe, K. (2012). Autophagic activity in thymus and liver during aging. *Age* 34, 75–85. doi: 10.1007/s11357-011-9221-9

- Ventevogel, M. S., and Sempowski, G. D. (2013). Thymic rejuvenation and aging. *Curr. Opin. Immunol.* 25, 516–522. doi: 10.1016/j.coi.2013.06.002
- Wang, Z., Gerstein, M., and Snyder, M. (2009). RNA-Seq: a revolutionary tool for transcriptomics. *Nat. Rev. Genet.* 10, 57–63. doi: 10.1038/nrg2484
- Xing, Y., and Hogquist, K. A. (2014). Isolation, identification, and purification of murine thymic epithelial cells. *J. Vis. Exp.* 90:e51780. doi: 10.3791/51780
- Xiong, C., Xie, C. Q., Zhang, L., Zhang, J., Xu, K., Fu, M., et al. (2005). Derivation of adipocytes from human embryonic stem cells. *Stem Cells Dev.* 14, 671–675. doi: 10.1089/scd.2005.14.671
- Yamamoto, S., Schulze, K. L., and Bellen, H. J. (2014). Introduction to Notch signaling. *Methods Mol. Biol.* 1187, 1–14. doi: 10.1007/978-1-4939-1139-4\_1
- Yang, H., Youm, Y. H., and Dixit, V. D. (2009). Inhibition of thymic adipogenesis by caloric restriction is coupled with reduction in age-related thymic involution. *J. Immunol.* 183, 3040–3052. doi: 10.4049/jimmunol.090562
- Youm, Y. H., Yang, H., Amin, R., Smith, S. R., Leff, T., and Dixit, V. D. (2010). Thiazolidinedione treatment and constitutive-PPARgamma activation induces ectopic adipogenesis and promotes age-related thymic involution. *Aging Cell* 9, 478–489. doi: 10.1111/j.1474-9726.2010.00574.x
- Youm, Y. H., Yang, H., Sun, Y., Smith, R. G., Manley, N. R., Vandanmagsar, B., et al. (2009). Deficient ghrelin receptor-mediated signaling compromises thymic stromal cell microenvironment by accelerating thymic adiposity. *J. Biol. Chem.* 284, 7068–7077. doi: 10.1074/jbc.M808302200
- Zhang, Y., Zeng, X., and Jin, S. (2012). Autophagy in adipose tissue biology. *Pharmacol. Res.* 66, 505–512. doi: 10.1016/j.phrs.2012.09.004
- Zhao, S., Fung-Leung, W. P., Bittner, A., Ngo, K., and Liu, X. (2014). Comparison of RNA-Seq and microarray in transcriptome profiling of activated T cells. *PLoS One* 9:e78644. doi: 10.1371/journal.pone.0078644

**Conflict of Interest Statement:** The authors declare that the research was conducted in the absence of any commercial or financial relationships that could be construed as a potential conflict of interest.

Copyright © 2018 Wang, Tan, Du, Liu, Wang, Wu, Yuan and Zhu. This is an open-access article distributed under the terms of the Creative Commons Attribution License (CC BY). The use, distribution or reproduction in other forums is permitted, provided the original author(s) and the copyright owner(s) are credited and that the original publication in this journal is cited, in accordance with accepted academic practice. No use, distribution or reproduction is permitted which does not comply with these terms.